El Malki et al.

Theoretical study of New Donor-π-Acceptor compounds based on Carbazole, Thiophene and Benzothiadiazole for Photovoltaic application as Dye-sensitized solar cells

Z. El Malki[1,*], M. Bouachrine[1], M. Hamidi[2], F. Serein-Spirau[3], J. P. Lere-Porte[3], J. Marc Sotiropoulos[4]

[1]MEM, ESTM, Université Moulay Ismaïl, Meknès, Maroc.
[2] URMM/UCTA, FST Errachidia, Maroc.
[3] Heterochimie Moléculaire et Macromoléculaire, UMR, CNRS 5076, Ecole Nationale Supérieure de Chimie de Montpellier, Montpellier, France.
[4] Université de Pau et des Pays de l'Adour, UMR5254 – IPREM, Equipe Chimie-Physique, Helioparc –Pau, France.

Abstract

In this study, we have designed a series of novel double organic D-π-A (electron donor-π-conjugated-acceptor) based on Carbazole, Thiophene and Benzothiadiazole. The optimized structures and optoelectronic properties of these dyes have been investigated by using the Density Functional Theory DFT/B3LYP/6-31G (d,p) method and Time Dependant Density Functional Theory (TD/DFT) calculations. These dyes consist of electron-donor (Carbazole-3,4-Ethylenedioxythiophene) and-acceptors/anchoring (Benzothiadiazole and Cyanoacrylic), connected by the π-conjugated linker as an electron donor spacer constituted of Thiophene and Phenylene units.
The calculated geometries indicate that these dyes have coplanar structures. The LUMO and HOMO energy levels of these dyes can ensure positive effect on the process of electron injection and dye regeneration. In order to predict the band gaps for guiding the synthesis of novel materials with low band gaps, we apply quantum-chemical techniques to calculate the band gaps in several oligomers. The trend of the calculated HOMO–LUMO (E_{gap}) gaps nicely compares with the spectral optical data. A low band gap will be expected in polymers containing double donor-acceptor (D-A) repeating units. The bridging effect by $C=C(CN)_2$ on the optoelectronic properties of the studied compounds is investigated. The calculated results of these dyes demonstrate that these compounds can be used as potential sensitizers for TiO_2 nanocrystalline solar cells.

Keywords: Benzothiadiazole; Carbazole; Tiophene; TD/DFT calculations; Donor-Acceptor; bridging effect.

1. Introduction

Dye-sensitized solar cells (DSSCs) have attracted so much attention due to their potential applications in coating and fabrication technologies because of their low cost and high photoelectric conversion efficiency [1–3]. Much of the combined research efforts have been directed toward developing materials that are application stable in the conducting state, easily processable, and relatively simple to produce at low cost. Light absorption in polymer solar cells leads to the generation of excited, bound electron–hole pairs or excitons. The interaction between the electron donor (D) and acceptor (A) moieties in such an alternating donor-acceptor copolymer can result in the hybridization of the high-lying HOMO energy level of the donor and low-lying energy levels of the acceptor, leading to a relatively small band gap polymer semiconductor with novel electronic structure. In recent years, interest in metal-free organic dyes as an alternative to noble metal complexes has increased due to their numerous advantages, such as the diversity of molecular structures, high molar extinction coefficients, simple synthesis, as well as low cost and environmental concerns. Many organic dyes, based on the donor (π spacer)-acceptor (D-π-A) system, exhibiting relatively high DSSC performance, have so far been designed and developed. They include

triarylamine dyes [4-7], hemicyanine dyes [8, 9], thiophene-based dyes [10], indoline dyes [11-14], and phthalocyanine [15] dyes. Although remarkable progress has beenmade in the development of organic dyes as sensitisers for DSSCs, optimising their chemical structures is required for further improvements in performance. TiO_2 can be formed in several phases such as anatas, rutaile and broklit. There are some properties of TiO_2 nano-crystal such as electroopticality, low cost, chemical stability, nontoxicity, abundance, availability and lack of erosion and corrosion against light which are common in the literature [16]. Tian et al. have reported a series of donor-acceptor-π-bridge-acceptor (D-A-π-A) structural organic dyes incorporating Benzotiadiazole into the triphenylamine framework, resulting in red-shift in absorption and weakening the deprotonation effect on TiO_2 film, which is beneficial for light-harvesting [17]. Several (3, 4-Ethylenedioxythiophene) (Edot) based donor–acceptor conjugated polymers with small band gaps have been reported [18-20]. On the other hand, most recent papers are focused on the Carbazole (Cbz) [21-23], due to its important specific properties (photoconductivity, photoluminescence and hole transport properties).

In this work, we report a theoretical study of the structural, electronic structures and the optical properties of (Carbazole-3,4 Ethylenedioxythiophene)-Benzotiadiazole [(Cbz-Edot)-B] based alternating donor conjugated oligomers constituted of thiophene (T) and phenylene (P) units. The cyanoacrylic acid (A) anchoring group leads to more red shift of absorption and emission bands. The molecular structures are shown in Figure. 1. The geometric structures and electronic properties were investigated by the density functional theory (DFT) at the B3LYP level and 6-31G(d, p) basis set. The researchers were interested in the structural modification of organic dye molecules by investigating the effect of different π spacer. Firstly, we studied the effects of the insertion of thiophene (T) and phenylene (P) units on the compounds; secondly, we analyzed the effects of the geometry and electronic properties of the conjugated copolymers due to long-side chains and finally, we examined the insertion effect of bridging by C=C $(CN)_2$ groups on the energy gaps and the electronic properties of the (Cbz-Edot)$_2$BTC=C(CN)$_2$TA copolymers. The calculated results were compared with the study's experimental data [24]. The results are a useful guide for the design, synthesis, and confirmation of the experiment.

2. Computational methods

In the present work, the ground-state geometries were fully optimized using a DFT level with the B3LYP hybrid functional [25-27]. All optimizations were calculated without any symmetry constraints using 6-31G (d,p) basis set on Gaussian 09 software package [28]. None of the frequency calculations generating imaginary frequencies indicate that the optimized geometries are true energy minima. The HOMO, LUMO and gap (HOMO-LUMO) energies are also deduced for the stable structures. We investigated the localization of the frontier orbitals. The spatial distribution of the frontier orbitals (HOMO) and (LUMO) provides a strategy by which the photovoltaic properties of solar cell can be understood. The vertical excitation energy, the wave lengths, and the electronic transition energies of the oligomers were obtained by using time-dependent density functional theory TD/DFT with B3LYP calculations. The electronic absorption and emission spectra of the dyes are calculated and simulated with TD/DFT method at the B3LYP/6-31G (d, p) level in vacuum.

3. Results and discussion

3.1 Geometrical parameters

The selected dihedral angle (θ) and bond distance (d) parameters of the optimized molecular structures are collected in Table 1. The dihedral angles of (Cbz-Edot)BPA, (Cbz-Edot)$_2$BPA and (Cbz-Edot)$_2$BP$_2$A which have phenylene-phenylene as π-spacer (PP) dyes and phenylene-acceptor moieties as π-spacer (PA) dyes were computed to be -25.55°, -25.87°, 34.51° and -25.69° respectively, and the dihedral angles of (Cbz-Edot)BTA, (Cbz-Edot)$_2$BTA, (Cbz-Edot)$_2$BT$_2$A and (Cbz-Edot)$_2$BT$_3$A which have thiophene-thiophene as π-spacer (TT) dyes and thiophene-acceptor moieties as π-spacer (TA) dyes were computed to be in the range of 174–180°. This can be explained by the fact that inserting a phenylene unit into the dye molecules directly causes the coplanarity of the structure to be more twisted due to the high repulsion force of NBO charges between the H atom on the phenylene ring and the H atom on the adjacent thiophene ring. This repulsion does not appear in TT dyes. It can be confirmed that the π-conjugated bridge in these (TT) dyes should be more planar and therefore the electron can be smoothly injected from the (Cbz-Edot) donor to the cyanoacrylic acceptor. The inter-ring distance is found to be about 1.42 Å for (TA) dyes, 1.45 Å for (CE-B) and (B-T) dyes, and 1.46 Å for (CE-CE). The dihedral angles formed between thiophene and cyanoacrylic acceptor plane in (Cbz-Edot)$_2$BT(C=C(CN)$_2$)TA are (-0.13°), the conjugated molecule is more planar, which explains the effect of the bridging system on the structure.

J. Mater. Environ. Sci. 7 (9) (2016) 3244-3255
ISSN : 2028-2508
CODEN: JMESC

El Malki et al.
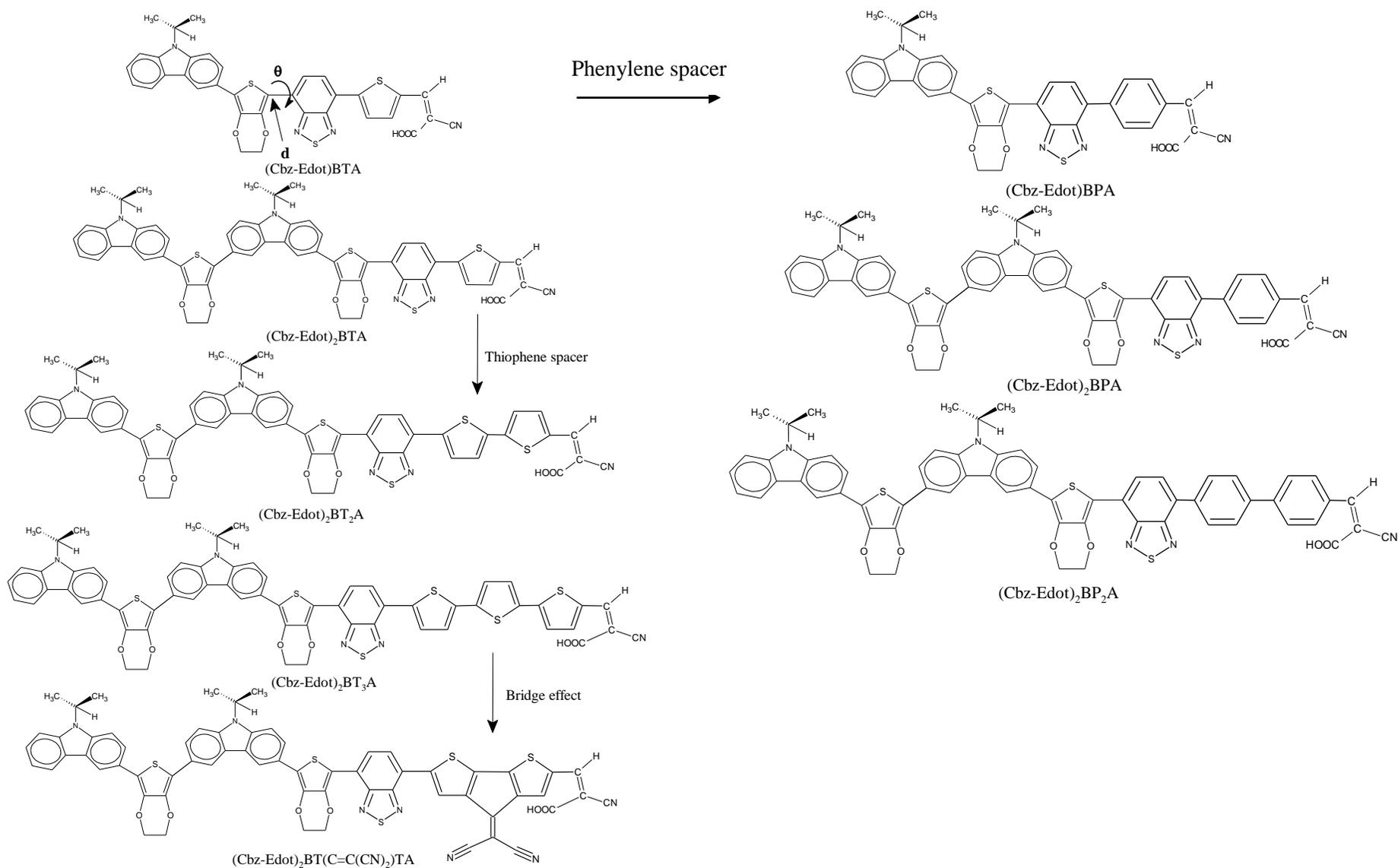
Figure 1: The sketch map structures of studied organic dyes.

The optimized geometries of lowest singlet excited states obtained using the CIS/3-21G* method are compared with their ground state structures. It can be seen that the inter-ring distances are shortened and found to be about 1.42 Å for (B-T) dyes and the dihedral angles are less than those in the ground state (-0.29°) for (B-T). These values suggest that in their relaxed excited state, all conformers acquire a quinoid form. That is, all molecules become more planar and possess a quinoid character in their lowest excited state (S_1). In the doped states, the compounds become more planar, show a quinoidal character and affect the electronic structure by lowering the energy band gap and raising conjugation length.

3.2 Energy gap

The energy gap (E_{gap}) for (Cbz-Edot)BPA, (Cbz-Edot)$_2$BPA, (Cbz-Edot)$_2$BP$_2$A, (Cbz-Edot)BTA, (Cbz-Edot)$_2$BTA, (Cbz-Edot)$_2$BT$_2$A, (Cbz-Edot)$_2$BT$_3$A and (Cbz-Edot)$_2$BT(C=C(CN)$_2$)TA was obtained by the differences of HOMO and LUMO energy levels ($\Delta E_{HOMO-LUMO}$) using B3LYP/6-31G(d,p). Table 2 lists the theoretical electronic property parameters (E_{HOMO}, E_{LUMO} and E_{gap}). Calculated band gaps were in the range of 1.01–2.25 eV. The calculated band gap E_{gap} of the studied compound increases in the following order : (Cbz-Edot)$_2$BT(C=C(CN)$_2$)TA (1.01 eV) < (Cbz-Edot)$_2$BT$_2$A (1.68 eV) < (Cbz-Edot)$_2$BTA (1.69 eV) < (Cbz-Edot)$_2$BT$_3$A (1.71 eV) < (Cbz-Edot)$_2$BPA (1.85 eV) < (Cbz Edot)$_2$BP$_2$A (1.95eV) < (Cbz-Edot)BTA (2.06 eV) < (Cbz-Edot)BPA (2.25 eV).

The (Cbz-Edot)$_2$BT(C=C(CN)$_2$)TA presents a lower band gap than the other studied materials due to the insertion of bridging system (C=C(CN)$_2$), resulting in an increase in the conjugation length of the molecule, promising better ICT properties. It was shown that in the comparison of (Cbz-Edot)BTA and (Cbz-Edot)BPA, the calculated E_{gap} of TA dye was computed to be 2.06 eV which increased to 2.25 eV for PA dye in the replacement of thiophene by the phenylene ring. Similarly, the E_{gap} of (Cbz-Edot)$_2$BT$_2$A, was calculated to be 1.68 eV and increased to 1.95 eV in (Cbz Edot)$_2$BP$_2$A. The results clearly indicated that inserting the phenylene unit at the position adjacent to the acceptor significantly increased the E_{gap}. It was shown that in the comparison of the experimental data of Cbz$_2$T$_2$A and Cbz$_2$T$_3$A [24] with the theoretical results of (Cbz-Edot)$_2$BT$_2$A and (Cbz-Edot)$_2$BT$_3$A, when we inserted the Edot and Benzothiadiazole units: the experimental E_{gap} of Cbz$_2$T$_2$A and Cbz$_2$T$_3$A were found to be 2.24 eV and 2.15 eV respectively, which decreased to 1.68 eV and 1.71 eV for (Cbz-Edot)$_2$BT$_2$A and (Cbz-Edot)$_2$BT$_3$A respectively. The results clearly indicated that inserting the (3,4-Ethylenedioxythiophene) unit at the position adjacent to the donor and inserting the Benzothiadiazole unit at the position adjacent to the acceptor decreased the E_{gap} significantly.

Table 2 shows detailed data of absolute energy of the frontier orbital for the studied molecules and TiO$_2$ are included for comparison purposes. It is deduced that the modification of structure pushes up/down the HOMO/LUMO energies in agreement with their electron donor/acceptor character. To evaluate the possibilities of electron transfer from the studied molecules to the conductive band of TiO$_2$, the HOMO and LUMO levels were compared (Figure. 2). Compared to the others, (Cbz-Edot)$_2$BT(C=C(CN)$_2$)TA, (Cbz-Edot)$_2$BT$_2$A, (Cbz-Edot)$_2$BTA and (Cbz-Edot)$_2$BT$_3$A contain respectively a bridging system and thiophene oligomers adjacent to the Benzothiadiazole and cyanoacetic acid groups, which decreases its LUMO, HOMO energy levels and decreases the energy gap, owing to their larger conjugation. Based on the above analysis, the LUMO energy levels of the eight dyes (-4.6 eV) are higher than that of ITO conduction band edge (−4.7 eV) [29]. As shown in Fig.2, both HOMO and LUMO levels of the studied molecules agree well with the requirement for an efficient photosentizer. Indeed, the LUMO levels are higher than the TiO$_2$ (-3.9 eV) [30, 31]. These driving forces are large enough for effective electron injection. Therefore, the studied dyes can be used as sensitizers because the electron injection process from the studied molecule to the conduction band of TiO$_2$ and the subsequent regeneration are feasible in organic sensitized solar cell. In organic solar cells, the open circuit voltage is found to be linearly dependent on the HOMO level of the donor and the LUMO level of the acceptor [32, 33]. The power conversion efficiency (PCE) was calculated according to the following Eq. (1):

$$P_{CE} = \frac{FF.V_{OC}.J_{SC}}{P_{in}} \tag{1}$$

Where P_{in} is the incident power density, J_{sc} is the short-circuit current, V_{oc} is the open-circuit voltage, and *FF* denotes the fill factor. To analyse the relationship between V_{OC} and E_{LUMO} of the dyes based on electron injection from LUMO to conduction band of TiO$_2$ (E_{cb}), the energy relationship can be expressed [34]:

$$V_{OC} = E_{LUMO}(Donor) - E_{cb}(TiO_2) \tag{2}$$

Table 1: Selected bond lengths (Å) and dihedral angles (degree) of optimized structures calculated by B3LYP/6-31G (d,p) level of theory.

Dyes						
		CE-B	**B-T**	**T-A**		
(Cbz-Edot)BTA	Distance (d)	1.452	1.455	1.424		
	Dihedral (θ)	- 42.12	2.59	-179.84		
		CE-CE	**CE-B**	**B-T**	**T-A**	
(Cbz-Edot)$_2$BTA	Distance (d)	1.463	1.452	1.455	1.424	
	Dihedral (θ)	22.92	-42.19	0.19	179.99	
		CE-CE	**CE-B**	**B-T**	**T-T**	**T-A**
(Cbz-Edot)$_2$BT$_2$A	Distance (d)	1.463	1.454	1.454	1.438	1.427
	Dihedral (θ)	23.30	-43.16	-0.92	178.14	-0.18
		CE-CE	**CE-B**	**B-T**	**T-T**	**T-T**	**T-A**
(Cbz-Edot)$_2$BT$_3$A	Distance (d)	1.464	1.455	1.454	1.439	1.437	1.423
	Dihedral (θ)	23.40	-43.42	1.64	174.57	-178.09	179.94
		CE-CE	**CE-B**	**B-T**	**T-A**		
(Cbz-Edot)$_2$BT(C=C(CN)$_2$)TA	Distance (d)	1.463	1.452	1.453	1.427		
	Dihedral (θ)	23.90	-41.82	1.64	-0.13		
		CE-B	**B-P**	**P-A**		
(Cbz-Edot)BPA	Distance (d)	1.455	1.476	1.457		
	Dihedral (θ)	-42.95	33.05	-25.55		
		CE-CE	**CE-B**	**B-P**	**P-A**	
(Cbz-Edot)$_2$BPA	Distance (d)	1.464	1.455	1.476	1.457	
	Dihedral (θ)	23.515	-43.16	32.94	-25.87	
		CE-CE	**CE-B**	**B-P**	**P-P**	**P-A**
(Cbz-Edot)$_2$BP$_2$A	Distance (d)	1.464	1.457	1.478	1.479	1.457
	Dihedral (θ)	23.91	-43.77	35.77	34.51	-25.69

Note: CE is (Carbazole-Edot), T is thiophene, P is phenylene, B is Benzothiadiazole and A is acceptor.

The theoretical values of the open circuit voltage V_{oc} / TiO_2 of the studied molecules range from 0.233 eV to 1.250 eV (Table 2). These values are sufficient for a possible efficient electron injection. Therefore, all the studied molecules can be used as sensitizers because the electron injection process from the excited molecule to the conduction band of the acceptor (TiO_2) and the subsequent regeneration is possible in organic sensitized solar cell.

The frontier molecular orbital (MO) contribution is very important in determining the charge-separated states of the studied molecules. The electronic structures of HOMO and LUMO of the eight molecules are shown in Figure. 3 and all these dyes have good electron-separated states. As shown in Fig.3, while strong localization of the HOMOs occurs on the (3,4-ethylenedioxythiophene) donor subunits of the polymer backbone, strong delocaliztion of the LUMOs occurs on the bridges between the subunits proving the flow of electron density along the polymer backbone. The electron density of LUMO is mainly localized on the acceptor units (mostly in the anchoring group), so the electronic transitions of of the studied molecules from HOMO to LUMO could lead to intramolecular charge transfer from the donor units to the anchoring groups through the conjugated bridge.

Table 2 : Energy values of the studied molecules calculated by B3LYP/6-31G (d,p) level.

| Studied compounds	E_{HOMO} (eV)	E_{LUMO} (eV)	E_{gap} (eV)	V_{oc} (eV)/TiO_2
(Cbz-Edot)BTA	-5.021	-2.953	2.068	0.947
(Cbz-Edot)$_2$BTA	-4.637	-2.947	1.690	0.953
(Cbz-Edot)$_2$BT$_2$A	-4.634	-2.948	1.686	0.952
(Cbz-Edot)$_2$BT$_3$A	-4.605	-2.891	1.714	1.009
(Cbz-Edot)$_2$BT(C=C(CN)$_2$)TA	-4.684	-3.667	1.017	0.233
(Cbz-Edot)BPA	-5.037	-2.786	2.251	1.114
(Cbz-Edot)$_2$BPA	-4.641	-2.782	1.859	1.118
(Cbz-Edot)$_2$BP$_2$A	-4.606	-2.650	1.956	1.250
TiO_2*		-3.900		

* Tian, et al ; (2010).
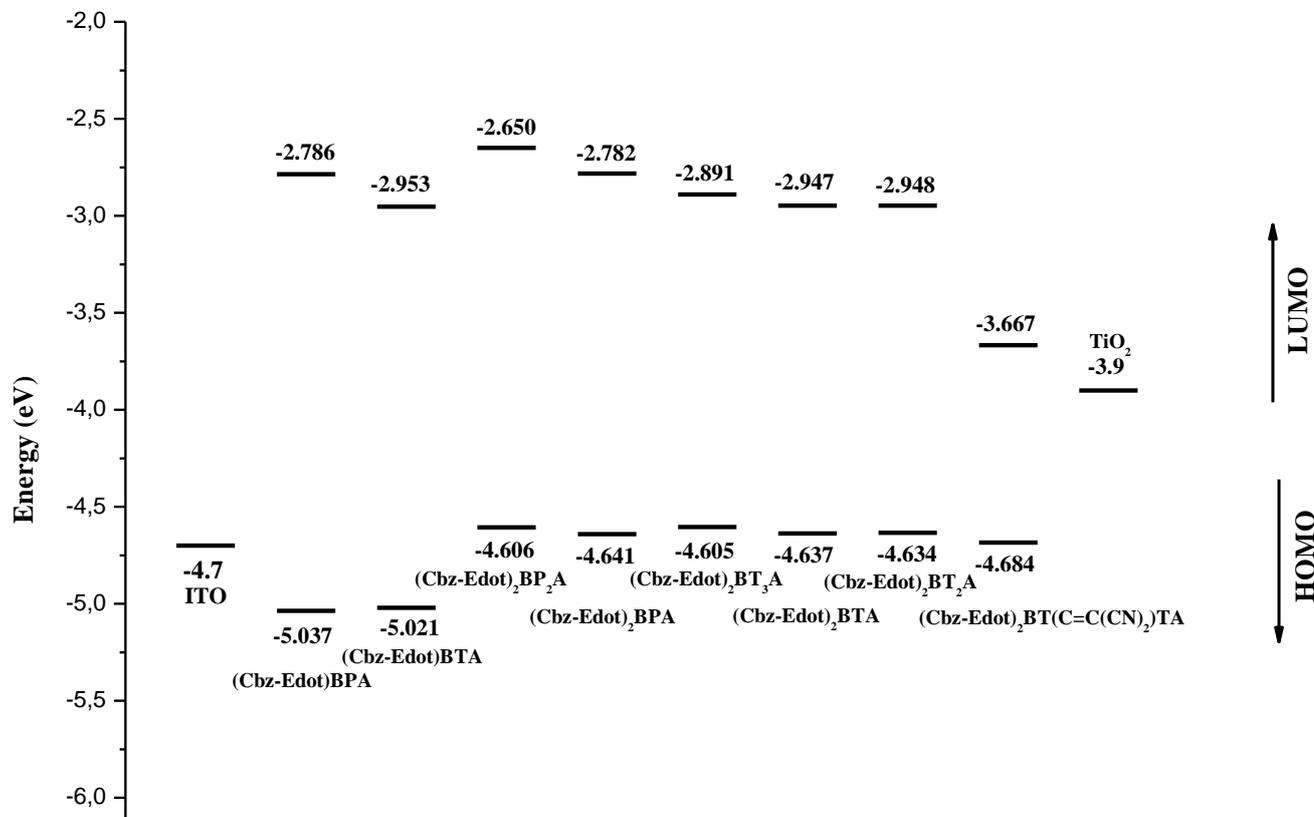
Figure 2 : Sketch of B3LYP/6-31 G (d,p) calculated energies of the
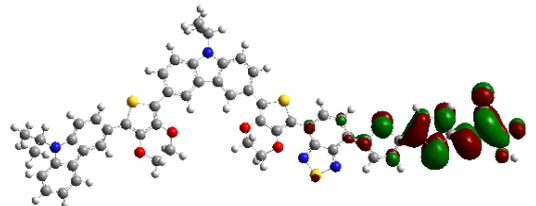HOMO and LUMO level of the studied molecules.

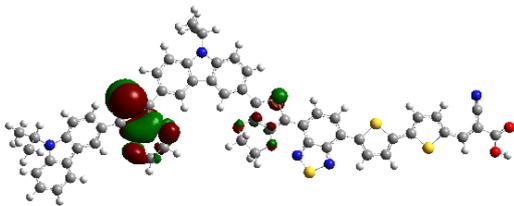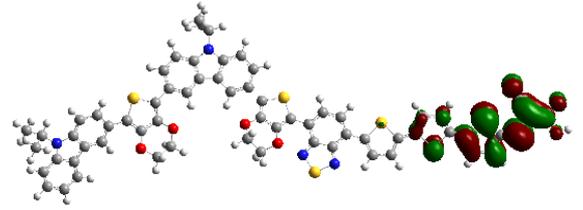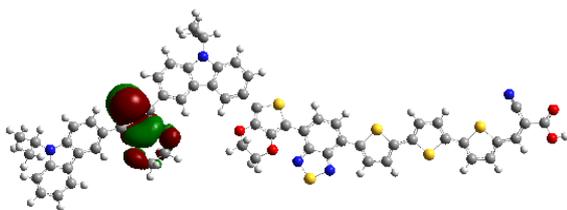HOMO   LUMO
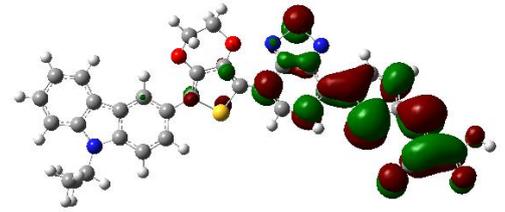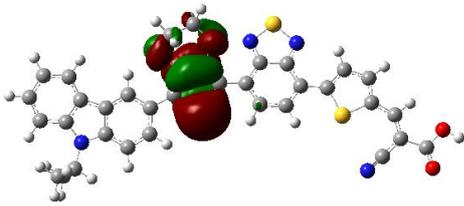
(Cbz-Edot)BTA
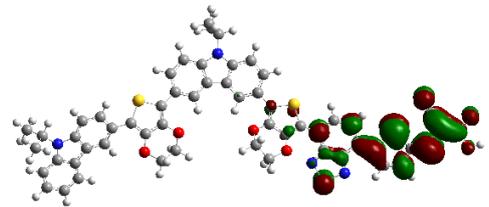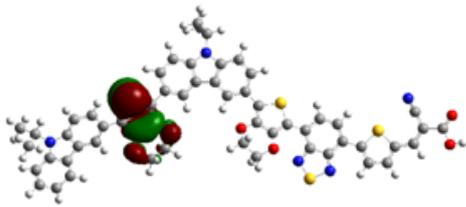
(Cbz-Edot) $_2$BTA

(Cbz-Edot) $_2$BT $_2$A

(Cbz-Edot) $_2$BT $_3$A

(Cbz-Edot) $_2$BT(C=C(CN) $_2$)TA

HOMO   LUMO


(Cbz-Edot)BPA
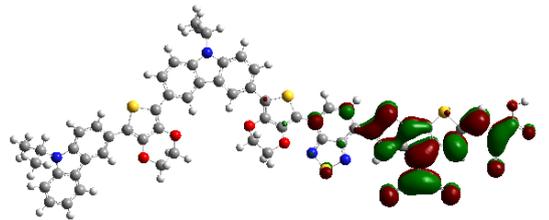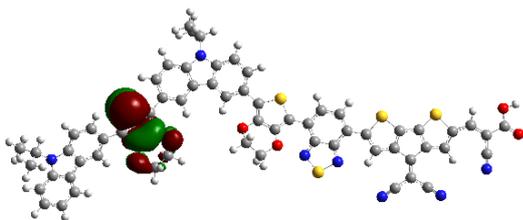
(Cbz-Edot)$_2$BPA

(Cbz Edot)$_2$BP$_2$A
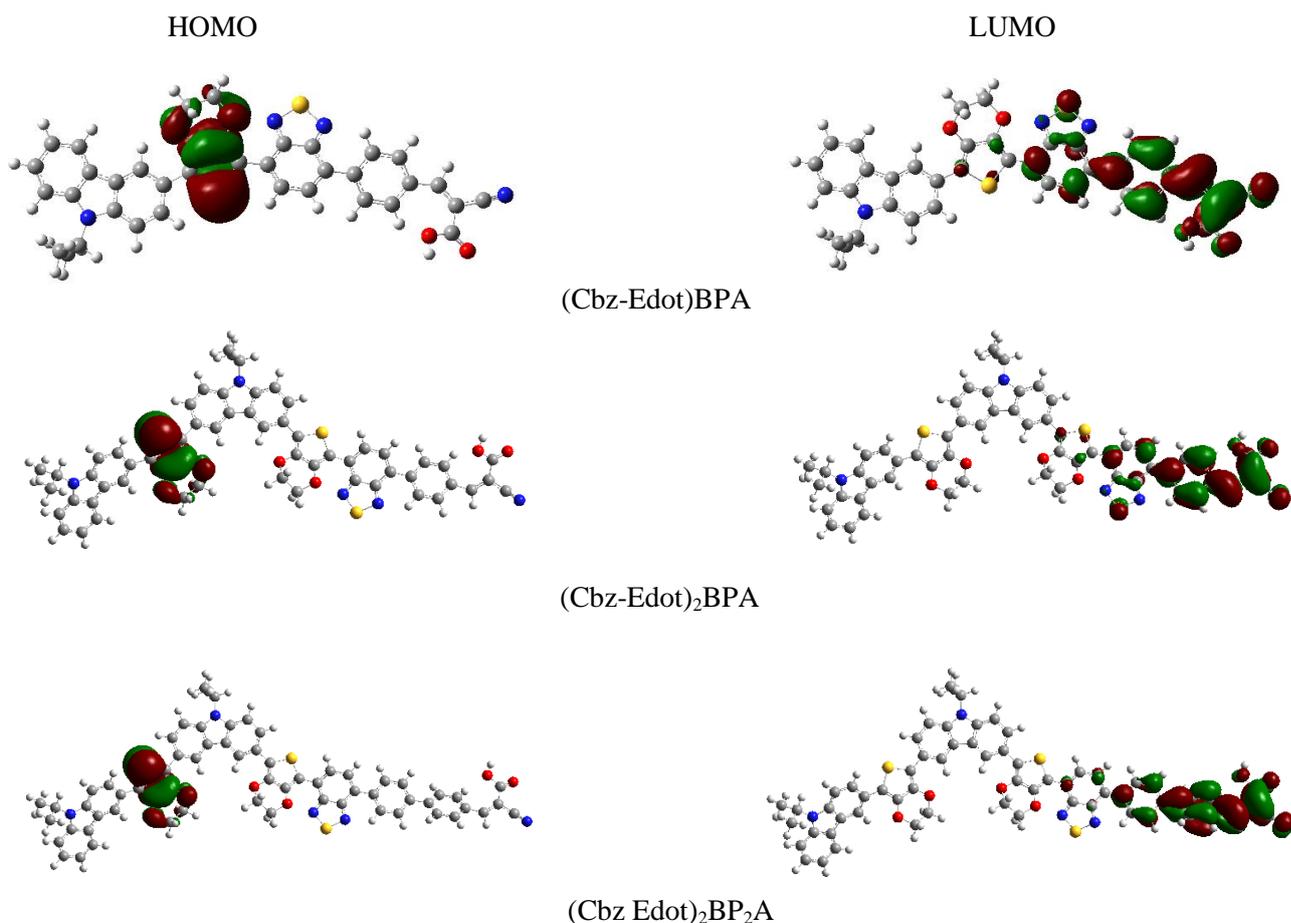
Figure 3 : The contour plots of HOMO and LUMO orbitals of the studied compounds.

3.3 UV/Vis absorption spectra
How the absorption of a new material matches with the solar spectrum is an important factor for the application as a photovoltaic material, and a good photovoltaic material should have broad and strong visible absorption characteristics. To gain insight of the optical property and electronic transition, the excitation energy and UV/Vis absorption spectra for the singlet-singlet transition of all sensitized dyes were simulated using TD/DFT method starting with optimized geometry obtained by B3LYP/6-31G(d,p) level. We present in Table 3 the vertical excitation energy E_{ex} (eV), calculated absorption λ_{max} (nm), oscillator strength (O.S) and molecular orbital character (MO/character) along with the main excitation configuration of all compounds. The obtained results demonstrate that the lowest singlet electronic excitation is characterized as a typical π-π* transition. The simulated absorption spectra of these dyes are shown in Figure. 4. (Cbz-Edot)$_2$BT$_2$A shows a series of bands between 623.62 and 675.31 nm, and the strongest absorption at **822.08** nm belonging to the HOMO to LUMO transition, (Cbz-Edot)$_2$BT$_3$A depicts a series of bands between 650.74 and 679.85 nm, and the absorption at **799.18** nm could be assigned to the electronic transition from HOMO to LUMO. (Cbz-Edot)$_2$BT(C=C(CN)$_2$)TA puts forward a series of bands between 776.56 nm and 1035.83 nm, and the absorption at **1428.12** nm is attributed to the electronic transition from HOMO to LUMO. In fact, the simulated absorption spectra (Fig. 4) show that all the studied compounds absorb from the UV/Vis, arises from delocalized π-π* transition in the polymer. Excitation to the S$_1$ state corresponds exclusively to the promotion of an electron from the HOMO to the LUMO. The absorption wavelengths arising from S$_0$ to S$_1$ electronic transition increase progressively with the increasing conjugation lengths. We have noted that introducing the C=C(CN)$_2$ group into oligomers backone affects the electronic structure by donating charge carriers thereby lowering the energy band gap and raising the conjugation length.

Table 3 : Absorption spectrum data obtained by TD/DFT methods for the compounds at B3LYP/6-31G(d,p) optimized geometries.

| Compounds	Elecrtronic transitions	λ_{abs} (nm)	E_{ex} (eV)	O.S	MO/character
(Cbz-Edot)BTA	$S_0 \longrightarrow S_1$	683.79	1.8132	0.6978	H $\longrightarrow$ L (70%)
	$S_0 \longrightarrow S_2$	511.38	2.4245	0.0313	H-1 $\longrightarrow$ L (48%)
	$S_0 \longrightarrow S_3$	488.13	2.5400	0.1353	H-1 $\longrightarrow$ L (46%)
(Cbz-Edot)$_2$BTA	$S_0 \longrightarrow S_1$	829.00	1.4956	0.1700	H $\longrightarrow$ L (70%)
	$S_0 \longrightarrow S_2$	662.59	1.8712	0.6419	H-1 $\longrightarrow$ L (69%)
	$S_0 \longrightarrow S_3$	550.87	2.2507	0.0031	H $\longrightarrow$ L+1(68%)
(Cbz-Edot)$_2$BT$_2$A	$S_0 \longrightarrow S_1$	822.08	1.5082	0.2224	H $\longrightarrow$ L (70%)
	$S_0 \longrightarrow S_2$	675.31	1.8360	0.8472	H-1 $\longrightarrow$ L (68%)
	$S_0 \longrightarrow S_3$	623.62	1.9881	0.0025	H $\longrightarrow$ L+1(68%)
(Cbz-Edot)$_2$BT$_3$A	$S_0 \longrightarrow S_1$	799.18	1.5514	0.2925	H $\longrightarrow$ L (69%)
	$S_0 \longrightarrow S_2$	679.85	1.8237	1.0186	H-1 $\longrightarrow$ L (62%)
	$S_0 \longrightarrow S_3$	650.74	1.9053	0.0288	H $\longrightarrow$ L+1(64%)
(Cbz-Edot)$_2$BT(C=C(CN)$_2$)TA	$S_0 \longrightarrow S_1$	1428.12	0.8682	0.0653	H $\longrightarrow$ L (70%)
	$S_0 \longrightarrow S_2$	1035.83	1.1970	0.2024	H-1 $\longrightarrow$ L (67%)
	$S_0 \longrightarrow S_3$	776.56	1.5966	0.1674	H $\longrightarrow$ L+1(69%)
(Cbz-Edot)BPA	$S_0 \longrightarrow S_1$	634.66	1.9535	0.5709	H $\longrightarrow$ L (69%)
	$S_0 \longrightarrow S_2$	505.58	2.4523	0.0045	H $\longrightarrow$ L+1(68%)
	$S_0 \longrightarrow S_3$	463.79	2.6733	0.1045	H-1 $\longrightarrow$ L (61%)
(Cbz-Edot)$_2$BPA	$S_0 \longrightarrow S_1$	746.41	1.6611	0.1572	H $\longrightarrow$ L (70%)
	$S_0 \longrightarrow S_2$	614.38	2.0180	0.5022	H-1 $\longrightarrow$ L (68%)
	$S_0 \longrightarrow S_3$	566.19	2.1898	0.0038	H $\longrightarrow$ L+1(69%)
(Cbz-Edot)$_2$BP$_2$A	$S_0 \longrightarrow S_1$	694.60	1.7850	0.1611	H $\longrightarrow$ L (68%)
	$S_0 \longrightarrow S_2$	616.35	2.0116	0.1061	H $\longrightarrow$ L+1(65%)
	$S_0 \longrightarrow S_3$	586.19	2.1151	0.3788	H-1 $\longrightarrow$ L (63%)
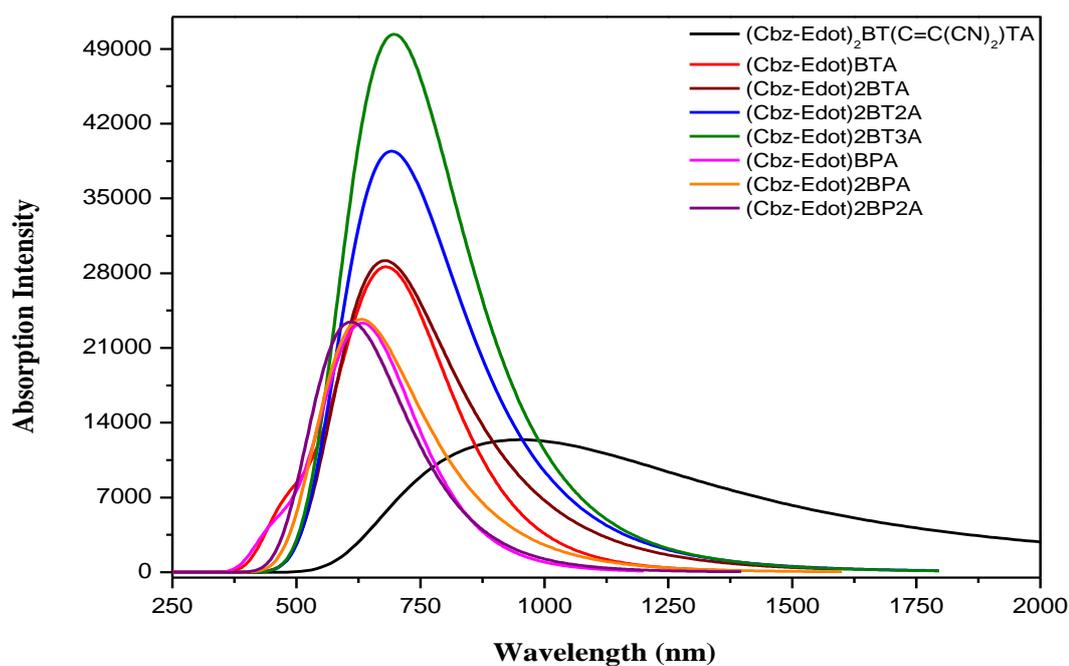
Figure 4 : Simulated UV-Visible optical absorption spectra of the studied compounds calculated by TD/DFT/B3LYP/6-31G (d, p) level.

3.4. Emission spectra

In order to study the emission photoluminescence properties of the studied compounds, the TD/B3LYP method is applied to the geometry of the lowest singlet excited state optimized at the CIS level with 3-21G* basis set. The emission spectrum of this copolymer is depicted in Figure. 5 and their corresponding emission parameters are summarized in Table 4. The predicted emission spectra are located in red visible light region (> 608 nm) with a maximum at about 1300 nm. This could be regarded as an electron transition process that is the reverse of the absorption corresponding mainly to the LUMO–HOMO-1 electron transition configuration.

The maximum emission peak is assigned to $S_1 \longrightarrow S_0$ transition as indicated in Table 4. We could also note that relatively low values of Stokes shift (SS) are obtained for (Cbz-Edot)$_2$BT(C=C(CN)$_2$)TA (277.84 nm). In fact, the stokes shift, defined as the difference between the absorption and emission maximums |EVA–EVE|, is related to the band widths of both absorption and emission bands [35]. (Cbz-Edot)$_2$BT(C=C(CN)$_2$)TA copolymer shows a greater stokes shift than (Cbz-Edot)$_2$BT$_3$A, (Cbz-Edot)$_2$BT$_2$A, (Cbz-Edot)$_2$BTA, (Cbz-Edot)BTA, (Cbz-Edot)$_2$BP$_2$A, (Cbz-Edot)$_2$BPA and (Cbz-Edot)BPA (277.84 nm versus 91.72 nm, 114.15 nm, 151.37 nm, 75.45 nm, 141.38 nm, 163.19 nm and 25.2 nm respectively) suggesting a higher degree of planarity in the exited state [36].
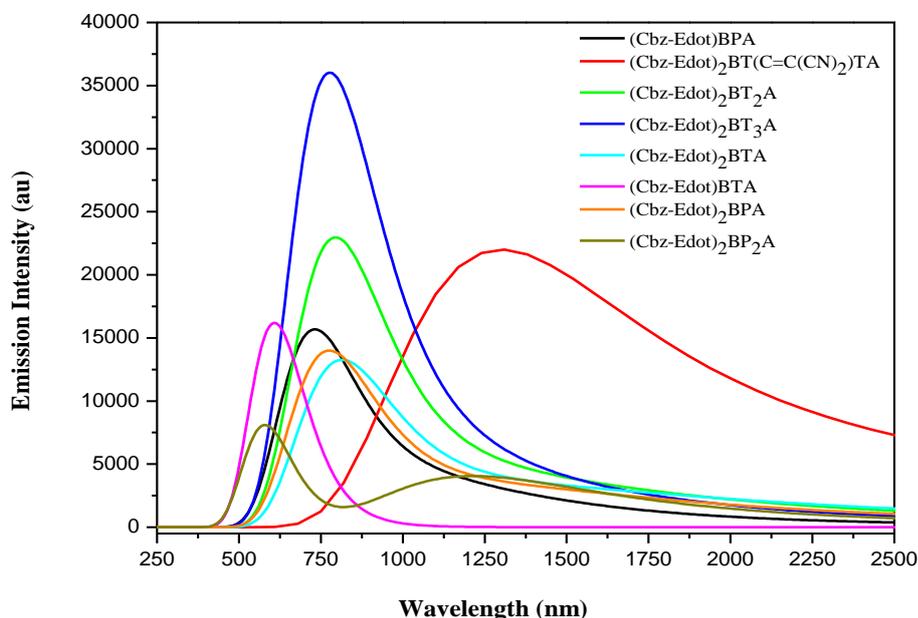
Figure 5 : Simulated emission spectra of the studied compounds calculated by TD/DFT/B3LYP level using CIS/3-21G* optimized geometries.

Table 4: Emission wavelengths, oscillator strengths computed with the TD/DFT level using CIS/3-21G* optimized geometries of the studied compounds.

Molecules	$\lambda_{Emission}$ (nm)	E_{ex} (eV)	O.S	MO % Contribution
(Cbz-Edot)BTA	608.34	2.04	0.512	HOMO $\longleftarrow$ LUMO (69.95)
(Cbz-Edot)$_2$BTA	813.96	1.52	0.313	HOMO-1 $\longleftarrow$ LUMO (68.55)
(Cbz-Edot)$_2$BT$_2$A	789.46	1.57	0.542	HOMO-1 $\longleftarrow$ LUMO (68.34)
(Cbz-Edot)$_2$BT$_3$A	771.57	1.61	0.857	HOMO-1 $\longleftarrow$ LUMO (68.01)
(Cbz-Edot)$_2$BT(C=C(CN)$_2$)TA	1313.67	0.94	0.51	HOMO-1 $\longleftarrow$ LUMO (68.63)
(Cbz-Edot)BPA	659.86	1.87	0.21	HOMO-1 $\longleftarrow$ LUMO (69.72)
(Cbz-Edot)$_2$BPA	777.57	1.59	0.27	HOMO-1 $\longleftarrow$ LUMO (62.65)
(Cbz-Edot)$_2$BP$_2$A	727.57	1.70	0.38	HOMO-1 $\longleftarrow$ LUMO (67.62)

Conclusion

In the present work, the structural and optical properties of a series of novel double organic D-π-A (electron donor-π-conjugated-acceptor) were efficiently studied by using DFT/TDDFT method. The calculated geometries indicate that the strength of the conjugation effects are formed in the studied compounds and the molecules are all planar. The systems have a quinoid character in their excited state. Based on the ground state geometry, it was found that the thiophene bridge in the compounds performed coplanar structure while the phenylene dyes were more twisted, therefore the electron in thiophene dyes can be efficiently injected from the donor to the acceptor of dye molecules. The E_{gap} energy gaps of (Cbz-Edot)BTA, (Cbz-Edot)$_2$BTA, (Cbz-Edot)$_2$BT$_2$A, (Cbz-Edot)$_2$BT$_3$A, and (Cbz-Edot)$_2$BT(C=C(CN)$_2$)TA were calculated to be 2.068, 1.690, 1.686, 1.714, and 1.017 eV respectively. The absorption bands of (Cbz-Edot)BTA, (Cbz-Edot)$_2$BTA, (Cbz-Edot)$_2$BT$_2$A, (Cbz-Edot)$_2$BT$_3$A, and (Cbz- Edot)$_2$BT(C=C(CN)$_2$)TA was found to be red-shifted compared to others. The HOMO state density is distributed entirely over all the conjugated molecules; while the shapes of the LUMO are localized on the Benzothiadiazole acceptor units.

Finally, the calculated results of these compounds demonstrate that these molecules can be used as potential sensitizers for TiO$_2$ nanocrystalline solar cells. We are also convinced that the systematic use of this theoretical approach presents a guiding tool to the synthesis process and helps to understand the structure-properties relationship of these new systems.

References

1. Gratzel M., *Nature* 414 (2001) 338–344.
2. Gratzel M., *J. Photochem. Photobiol*. C 4 (2003) 145–153.
3. Argazzi R., Iha N.Y.M., Zabri H., Odobel F., Bignozzi C.A., *Coord. Chem. Rev*. 248 (2004) 1299–1316.
4. Ning Z., Tian H., *Chem Commun.* (2009) 5483-95.
5. Lee D.H., Lee M.J., Song H.M., Song B.J., Seo K.D., Kim H.K., et al. *Dyes Pigments.* 91 (2011) 192-8.
6. Ning Z., Zhang Q., Wu W., Pei H., Liu B., Tian H., *J. Org. Chem.* 73 (2008) 3791-7.
7. Li G., Jiang KJ., Li YF., Li SL., Yang LM., *J. Phys. Chem.* C 112 (2008) 11591-9.
8. Wang Z.S., Li F.Y., Huang C.H., Wang L., Wei M., Jin L.P., et al., *J. Phys. Chem.* B 104 (2000) 9676-82.
9. Chen Y.S., Li C., Zeng Z.H., Wang W.B., Wang X.S., Zhang B.W., *J. Mater. Chem.* 15 (2005) 1654-61.
10. Tanaka K., Takimiya K., Otsubo T., Kawabuchi K., Kajihara S., Harima Y., *Chem. Lett.* 35 (2006) 592-3.
11. Horiuchi T., Miura H., Uchida S., *J. Photochem Photobiol A Chem.* 164 (2004) 29-32.
12. Horiuchi T., Miura H., Sumioka K., Uchida S., *J. Am. Chem Soc.* 126 (2004) 12218-9.
13. Schmidt-Mende L., Bach U., Humphry-Baker R., Horiuchi T., Miura H., Ito S., Uchida S., Grätzel M., *Adv Mater.* 17 (7) (2005) 813-815.
14. Ito S., Zakeeruddin S.M., Humphry-Baker R., Liska P., Charvët R., Comte P., Nazeeruddin Md.K., Pechy P., Takata M., Miura H., Uchida S., Grätzel M., *Adv Mater.* 18 (2006) 1202-1205.
15. Eu S., Katoh T., Umeyama T., Matano Y., Imahori H., *Dalton Trans.* (2008) 5476-83.
16. Diebold U., *Appl. Phys*. A 76 (2003) 681.
17. Zhu W., Wu Y., Wang S., Li W., Wang Z., Tian H. *Adv Funct. Mater.* 21 (2010) 756-63.
18. Zhu SS., Swager T.M., *J. Am. Chem. Soc.* 119 (1997) 12568.
19. Huang H., Pickup P.G., *Chem. Mater.* 10 (1998) 2212.
20. Akoudad S., Roncali J., *Chem Commun* 9 (1998) 2081.
21. Zotti G., Schiavon G., Zecchin S., Morin J. F., Leclerc M., *Macromolecules.* 35 (2002) 2122.
22. Garnier F., Horowitz G., Peng X., Fichou D., *Adv.Mater* 2 (1990) 562.
23. E.Gill R., Malliaras G. G., Wildeman J., Hadziioannou G., *Adv. Mater* 6 (1994) 132.
24. Jianhui H., Hsiang-Yu C., Shaoqing Z., Gang L., Yang Y., *J. Am. Chem. Soc.*, 130 (48) (2008) 16144-16145.
25. Vosko C.H., Wilk L., Nusair M., Can. J. Phys. 58 (1980) 1200-1211.
26. Becke A.D., *J. Chem. Phys*. 98 (1993) 5648-5652.
27. Becke A.D., *Phys. Rev*. A 38 (1988) 3098-3100.

28. Frisch M.J., Trucks G.W., Schlegel H.B., Scuseria G.E., Robb M.A., Cheeseman J.R., Scalmani G., Barone V., Mennucci B., Petersson G.A., Nakatsuji H., Caricato M., LX. i, Hratchian H.P., Izmaylov A.F., Bloino J., Zheng G., Sonnenberg J.L., Hada M., Ehara M., Toyota K., Fukuda R., Hasegawa J., Ishida M., Nakajima T., Honda Y., Kitao O., Nakai H., Vreven T., Montgomery J.A., Peralta J.J.E., Ogliaro F., Bearpark M., Heyd J.J., Brothers E., Kudin K.N., Staroverov V.N., Kobayashi R., Normand J., Raghavachari K., Rendell A., Burant J.C., Iyengar S.S., Tomasi J., Cossi M., Rega N., Millam J.M., Klene M., Knox J.E., Cross J.B., Bakken V., Adamo C., Jaramillo J., Gomperts R., Stratmann R.E., Yazyev O., Austin A.J., Cammi R., Pomelli C., Ochterski J.W., Martin R.L., Morokuma K., Zakrzewski V.G., Voth G.A., Salvador P., Dannenberg J.J., Dapprich S., Daniels A.D., Farkas O., Foresman J.B., Ortiz J.V., Cioslowski J., Fox D.J., Gaussian 09, Gaussian Inc., Wallingford, CT, 2009.
29. Asbury J.B., Wang Y.Q., Hao E., Ghosh H., Lian T., *Res. Chem. Intermed*. 27 (2001) 393–406.
30. Wu Z., Fan B., Xue F., Adachi C., Ouyang J. *Sol. Energy Mater. Sol. Cells* 94 (2010) 2230.
31. Tian H., Yang X., Cong J., Chen R, Teng C., Liu J., Hao Y., Wang Lei., Sun L. *Dyes Pigm*. 84 (2010) 62.
32. Gadisa A., Svensson M., Andersson M.R., Inganas O. *Appl. Phys. Lett*. 84 (2004) 1609.
33. Scharber M.C., Mühlbacher D., Koppe M., Denk P., Waldauf C., Heeger A.J., Brabec C.J. *Adv. Mater*. 18 (2006) 789.
34. Sang Aroon W., Saekow S., Amornkitbamrung V. *J. Photochem. Photobiol., A : Chemistry* 236 (2012) 35–40.
35. Yu J.-S.K., Chen W.-C., Yu C.-H., *J. Phys. Chem*. A 107 (2003) 4268–4275.
36. Wang E., Wang M., Wang L., Duan C., Zhang J., Cai W., He C., Wu H., Cao Y., *Macromol.* 42 (2009) 4410–4415.